Available online at www.sciencedirect.com
SCIENCE DIRECT®
ELSEVIER Applied Mathematics and Computation 169 (2005) 485–499
APPLIED MATHEMATICS AND COMPUTATION
www.elsevier.com/locate/amc

Solving Laplacian problems with boundary singularities: a comparison of a singular function boundary integral method with the p/hp version of the finite element method

Miltiades Elliotis [a], Georgios Georgiou [a,*], Christos Xenophontos [b]

[a] *Department of Mathematics and Statistics, University of Cyprus, P.O. Box 20537, CY-1678 Nicosia, Cyprus*
[b] *Department of Mathematical Sciences, Loyola College, 4501 N. Charles Street, Baltimore MD 21210, USA*

Abstract

We solve a Laplacian problem over an L-shaped domain using a singular function boundary integral method as well as the *p/hp* finite element method. In the former method, the solution is approximated by the leading terms of the local asymptotic solution expansion, and the unknown singular coefficients are calculated directly. In the latter method, these coefficients are computed by post-processing the finite element solution. The predictions of the two methods are discussed and compared with recent numerical results in the literature.

Keywords: Laplace equation; Corner singularities; Stress intensity factors; Boundary integral method; Lagrange multipliers; *p/hp* finite element method

* Corresponding author.
E-mail address: georgios@ucy.ac.cy (G. Georgiou).

0096-3003/$ - see front matter
doi:10.1016/j.amc.2004.09.058

1. Introduction

In the past few decades, many different methods have been proposed for the numerical solution of plane elliptic boundary value problems with boundary singularities, aiming at improving the accuracy and resolving the convergence difficulties that are known to appear in the neighborhood of such singular points. These methods range from special mesh-refinement schemes to sophisticated techniques that incorporate, directly or indirectly, the form of the local asymptotic expansion, which is known in many occasions. In polar coordinates (r, θ) centered at the singular point, the local solution is of the general form

$$u(r, \theta) = \sum_{j=1}^{\infty} a_j r^{\mu_j} f_j(\theta), \tag{1}$$

where μ_j are the eigenvalues and f_j are the eigenfunctions of the problem, which are uniquely determined by the geometry and the boundary conditions along the boundaries sharing the singular point. The singular coefficients α_j, also known as generalized stress intensity factors [1] or flux intensity factors [2], are determined by the boundary conditions in the remaining part of the boundary. Knowledge of the singular coefficients is of importance in many engineering applications.

An exhaustive survey of treatment of singularities in elliptic boundary value problems is provided in the recent article by Li and Lu [3], who classify the proposed methods into three categories: methods involving local refinement, methods involving singular functions supplementing the approximation spaces of standard numerical methods, and combined methods which incorporate local singular and analytical solutions. A review of singular intensity factor evaluation and modelling of singularities in boundary integral methods is provided by Mukhopadhyay et al. [4].

In the Finite Element Method (FEM), which is the most commonly used method for solving structural mechanics problems, the singular coefficients are calculated by post-processing the numerical solution. Generally speaking, the most effective versions of the FEM are the high-order *p* and *hp* versions, in which instead of simply refining the mesh, convergence is achieved by: (i) increasing the degree of the piecewise polynomials in the case of the *p* version, and (ii) by increasing *p* and decreasing *h* in the case of the *hp* version. The reason for the success of these methods is that they are able to approximate singular components of the solution to elliptic boundary value problems (that arise, for example, at corners of the domain) very efficiently. For instance, the *hp* version, over appropriately designed meshes, approximates these singularities at an *exponential* rate of convergence [5]. Different solution post-processing methods for the calculation of the singular coefficients from the finite element solution have been proposed by Babuška and Miller [6,7], Szabó and Yosibash [8,9], and Brenner [10].

In the past few years, Georgiou and co-workers [11–13] developed the Singular Function Boundary Integral Method (SFBIM), in which the unknown singular coefficients are calculated directly. The solution is approximated by the leading terms of the local asymptotic solution expansion and the Dirichlet boundary conditions are weakly enforced by means of Lagrange multipliers. The method has been tested on standard Laplacian problems, yielding extremely accurate estimates of the leading singular coefficients, and exhibiting exponential convergence with respect to the number of singular functions.

The objective of the present paper is to compare the predictions of the SFBIM against those of the *p*/*hp* version of the FEM. We consider as a test problem the Laplacian problem over an *L*-shaped domain solved by Igarashi and Honma [14]. They used a modified version of the singular boundary integral method proposed by Symm [15]. The approximation of the solution around the singularity is expanded into a series of special harmonic functions and is regularized by subtracting the four leading terms of the local expansion. It is then calculated by the standard boundary element method. The accuracy of the calculated singular coefficients is restricted to five significant digits. As shown below, the predictions of both the SFBIM and the *p*/*hp*-FEM are of much higher accuracy.

The outline of the present paper is as follows: in Section 2, we present the SFBIM in the case of a general Laplacian problem over an arbitrary domain with a boundary singularity. In Section 3, the SFBIM is applied to the test problem. In Sections 4 and 5, the results of the SFBIM and the *p*/*hp*-FEM, respectively, are presented and discussed. Comparisons are also made with the results provided by Igarashi and Honma [14]. The conclusions are summarized in Section 6.

2. The singular function boundary integral method (SFBIM)

In order to present and formulate the singular function boundary integral method, we consider the rather general Laplace equation problem over a two-dimensional domain Ω, shown in Fig. 1. This is characterized by the presence of a boundary singularity at the corner O, formed by the straight boundary segments S_1 and S_2. With the exception of O, the boundary of Ω is everywhere smooth. In the remaining parts of the boundary, either Dirichlet or Neumann boundary conditions apply. Without loss of generality, the following problem is considered:

$$\nabla^2 u = 0 \quad \text{in } \Omega, \tag{2}$$

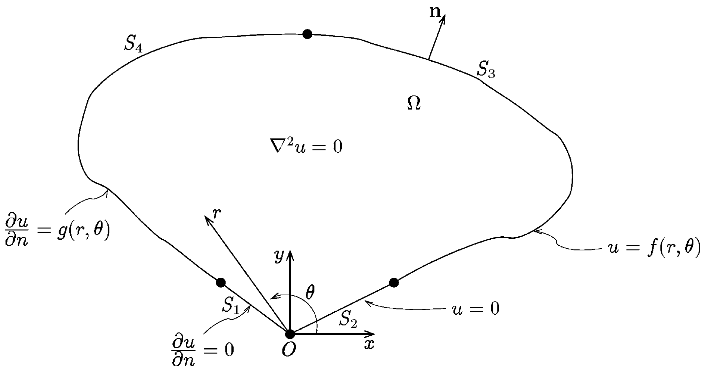

Fig. 1. A two-dimensional Laplace equation problem with one boundary singularity.

with

$$\left.\begin{array}{ll} \dfrac{\partial u}{\partial n} = 0 & \text{on } S_1 \\ u = 0 & \text{on } S_2 \\ u = f(r,\theta) & \text{on } S_3 \\ \dfrac{\partial u}{\partial n} = g(r,\theta) & \text{on } S_4 \end{array}\right\}, \tag{3}$$

where $\partial\Omega = S_1 \cup S_2 \cup S_3 \cup S_4$, and f and g are given functions such that no other boundary singularity is present.

The asymptotic solution in polar co-ordinates (r,θ) centered at the singular point, is given by [16]

$$u(r,\theta) = \sum_{j=1}^{\infty} \alpha_j r^{\mu_j} f_j(\theta), \quad (r,\theta) \in \Omega, \tag{4}$$

where α_j are the unknown singular coefficients, μ_j are the singularity powers arranged in ascending order, and the functions $f_j(\theta)$ represent the θ-dependence of the eigensolution.

The SFBIM [11–13] is based on the approximation of the solution by the leading terms of the local solution expansion:

$$\bar{u} = \sum_{j=1}^{N_\alpha} \bar{\alpha}_j W^j, \tag{5}$$

where N_α is the number of basis functions, and

$$W^j \equiv r^{\mu_j} f_j(\theta) \tag{6}$$

are the singular functions. It should be noted that this approximation is valid only if Ω is a subset of the convergence domain of the expansion (4). If not, it may still be possible to use this approach provided there exist (possibly different) expansions similar to (3) in different sectors of the domain Ω (see e.g. [17]).

Application of Galerkin's principle gives the following set of discretized equations:

$$\int_{\Omega} \nabla^2 u W^i \, \mathrm{d}V = 0, \quad i = 1, 2, \ldots, N_\alpha. \tag{7}$$

By using Green's second identity and taking into account that the singular functions, W^i, are harmonic, the above volume integral is reduced to a boundary one:

$$\int_{\partial\Omega} \left(\frac{\partial \bar{u}}{\partial n} W^i - \bar{u} \frac{\partial W^i}{\partial n} \right) \mathrm{d}S = 0, \quad i = 1, 2, \ldots, N_a. \tag{8}$$

The dimension of the problem is, thus, reduced by one, which leads to a considerable reduction of the computational cost. Since, now, W^i exactly satisfy the boundary conditions along S_1 and S_2, the above integral along these boundary segments is identically zero. Therefore, we have:

$$\int_{S_3} \left(\frac{\partial \bar{u}}{\partial n} W^i - \bar{u} \frac{\partial W^i}{\partial n} \right) \mathrm{d}S + \int_{S_4} \left(W^i \frac{\partial \bar{u}}{\partial n} - \bar{u} \frac{\partial W^i}{\partial n} \right) \mathrm{d}S = 0, \quad i = 1, 2, \ldots, N_a. \tag{9}$$

To impose the Neumann condition along S_4, we simply substitute the normal derivative by the known function g (Eq. (3)). The Dirichlet condition along S_3 is imposed by means of a Lagrange multiplier function, λ, replacing the normal derivative. The function λ is expanded in terms of standard, polynomial basis functions M^j,

$$\lambda = \frac{\partial \bar{u}}{\partial n} = \sum_{j=1}^{N_\lambda} \lambda_j M^j, \tag{10}$$

where N_λ represents the total number of the unknown discrete Lagrange multipliers (or, equivalently, the total number of Lagrange-multiplier nodes) along S_3. The basis functions M^j are used to weight the Dirichlet condition along the corresponding boundary segment S_3. We thus obtain the following system of $N_\alpha + N_\lambda$ discretized equations:

$$\int_{S_3} \left(\lambda W^i - \bar{u} \frac{\partial W^i}{\partial n} \right) \mathrm{d}S - \int_{S_4} \bar{u} \frac{\partial W^i}{\partial n} \mathrm{d}S = - \int_{S_4} W^i g(r, \theta) \, \mathrm{d}S,$$
$$i = 1, 2, \ldots, N_a, \tag{11}$$

$$\int_{S_3} \bar{u} M^i \, \mathrm{d}S = \int_{S_3} f(r, \theta) M^i \, \mathrm{d}S, \quad i = 1, 2, \ldots, N_\lambda. \tag{12}$$

It is easily shown that the linear system of Eqs. (11) and (12) is symmetric. This can be written in the following block form:

$$\begin{bmatrix} K_1 & K_2 \\ K_2^{\mathrm{T}} & O \end{bmatrix} \begin{bmatrix} A \\ \Lambda \end{bmatrix} = \begin{bmatrix} F_1 \\ F_2 \end{bmatrix}, \tag{13}$$

where A is the vector of the unknown singular coefficients, α_i, Λ is the vector of the unknown Lagrange multipliers λ_i, submatrices K_1 and K_2 contain the coefficients of the unknowns (obviously, K_1 is symmetric), and vectors F_1 and F_2 contain the RHS contributions of Eqs. (11) and (12), respectively. It should be noted that the integrands in Eq. (11) are non-singular and all integrations are carried out far from the boundaries causing the singularity.

3. Application of the SFBIM to a test problem

We consider the same Laplacian problem over an L-shaped domain as in [14], shown in Fig. 2. The local solution expansion around the singularity at $x = y = 0$ is given by

$$u = \sum_{j=1}^{\infty} \alpha_j r^{2(2j-1)/3} \sin\left[\frac{2}{3}(2j-1)\theta\right]. \tag{14}$$

Taking into account the symmetry of the problem, we consider only half of the domain and note that even-numbered coefficients are zero. Therefore, u may be written as follows:

$$u = \sum_{j=1}^{\infty} \alpha_j W^j, \tag{15}$$

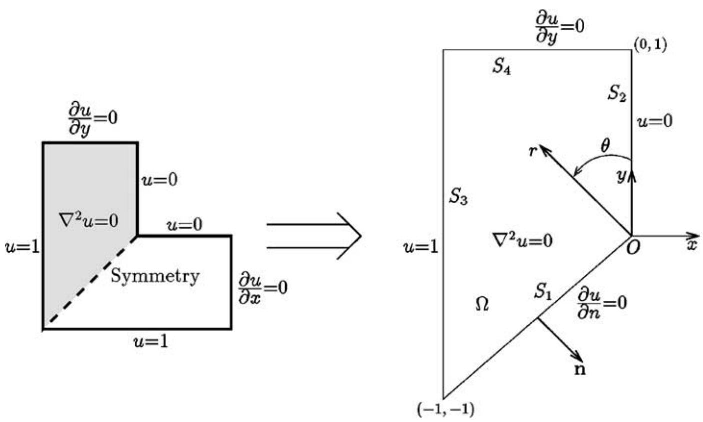

Fig. 2. Geometry and boundary conditions of the test problem.

where

$$W^j = r^{2(4j-3)/3} \sin\left[\frac{2}{3}(4j-3)\theta\right] \tag{16}$$

are the singular functions.

Setting $f = 1$ and $g = 0$, Eqs. (11) and (12) are simplified as follows:

$$-\int_{S_3}\left(\lambda W^i - \bar{u}\frac{\partial W^i}{\partial x}\right)\mathrm{d}y - \int_{S_4}\bar{u}\frac{\partial W^i}{\partial y}\,\mathrm{d}x = 0, \quad i = 1, 2, \ldots, N_\alpha, \tag{17}$$

$$\int_{S_3}\bar{u}M^i\,\mathrm{d}y = \int_{S_3}M^i\,\mathrm{d}y, \quad i = 1, 2, \ldots, N_\lambda. \tag{18}$$

In [14], the quantity

$$C := 2\int_{S_3\cup S_4}\frac{\partial u}{\partial n}\,\mathrm{d}S \tag{19}$$

referred to as the capacitance, was of interest. Note that due to the geometry and boundary conditions, (19) reduces to

$$C = -2\int_{-1}^{1}\left.\frac{\partial u}{\partial x}\right|_{x=-1}\mathrm{d}y. \tag{20}$$

4. Numerical results with the SFBIM

The Lagrange multiplier function λ used to impose the Dirichlet condition along S_3 is expanded in terms of quadratic basis functions. Boundaries S_3 and S_4 are subdivided, respectively, into $2N$ and N quadratic elements of equal size. Thus, the number of Lagrange multipliers is $N_\lambda = 4N + 1$. The integrals in Eqs. (17) and (18) involve singular functions that are not polynomial and become highly oscillatory as N_α increases. These are calculated numerically by subdividing each quadratic element into 10 subintervals and using a 15-point Gauss–Legendre quadrature over each subinterval. In computing the coefficient matrix, its symmetry is taken into account.

Several series of runs were performed in order to obtain the optimal values of N_α and N_λ. Our search was guided by the fact that N_λ should be large enough in order to assure accurate integrations along the boundary (which is divided into smaller elements) but much smaller than N_α in order to avoid ill-conditioning of the stiffness matrix. On the other hand, N_α cannot be very high, given that the computer accuracy cannot handle the contributions of the higher-order singular functions which become very small for $r < 1$ or very large for $r > 1$. Hence, N_λ was varied from 5 up to 65 and N_α from a value slightly above N_λ up to 100.

The convergence of the solution with the number of Lagrange multipliers is shown in Table 1, where we tabulate the values of the five leading singular coefficients and the capacitance C calculated with $N_\alpha = 60$. We observe that the values of the singular coefficients converge rapidly with N_λ, up to $N_\lambda = 41$, and that very accurate estimates are obtained. For higher values of N_λ, however, signs of divergence are observed, due to the ill-conditioning of the stiffness matrix. In addition to the divergence of the singular coefficients, another manifestation of ill-conditioning is the appearance of wiggles on the calculated Lagrange multiplier function [13]. The quality of the solution for $N_\alpha = 60$ and $N_\lambda = 41$ was checked by plotting λ as a function of y (Fig. 3) and verifying that λ is smooth and free of oscillations.

The values of the leading singular coefficients and the capacitance C calculated for $N_\lambda = 41$ and various values of N_α are shown in Table 2. Exponential convergence with respect to N_α is observed and extremely accurate estimates of the singular coefficients are obtained. Our calculations with different values of N_α and N_λ show that the optimal values are $N_\alpha = 60$ and $N_\lambda = 41$. In Table 3, the converged values of the singular coefficients calculated with these optimal choices of N_α and N_λ are presented. The CPU time required for the above run is 1.6 s on an IBM RS6000 (Processor type: Power PC 604e/375 MHz).

In Table 3, we see that the contributions of the higher-order terms are progressively vanishing. Note that the converged value of α_1 (1.12798040105939) is accurate to fifteen significant digits, while the value provided by Igarashi and Honma [14] (1.1280) is accurate only to five significant digits. The improved accuracy is also reflected on the calculated value of the capacitance, which is converged to eight significant digits, $C = 2.5585231$.

Finally, in Fig. 4, we plot the errors in the calculated values of the leading singular coefficients for $N_\alpha = 60$ versus the number of Lagrange multipliers. The errors are based on the converged values tabulated in Table 3. It is clear that the SFBIM converges exponentially with N_λ, and the error is reduced rapidly down to machine accuracy.

5. Numerical results with the *p*/*hp* version of the finite element method

In this section we present the results of solving the same test problem, using the *p*/*hp* version of the FEM over a geometrically graded mesh seen in Fig. 5. This is, to our knowledge, the most effective technique for approximating the solution to elliptic boundary value problems with corner singularities in the context of the FEM. We refer to [1] for more details on corner singularities and geometrically graded meshes in conjunction with the *p* and *hp* versions of the FEM. Once the solution u_{FEM} is obtained, the singular coefficients α_j, are computed as a post-solution operation. In particular, the algorithm for computing the α_j's is based on an L^2 projection of u_{FEM} into the space of func-

Table 1
Convergence of the solution with N_λ; SFBIM with $N_\alpha = 60$

N_λ	α_1	α_2	α_3	α_4	α_5	C
5	1.12797118414119	0.16993982990692	−0.02304003771255	0.00346892482591	0.00096430271538	2.5585187
9	1.12798030920688	0.16993376833638	−0.02304036610151	0.00346994177533	0.00091656933158	2.5585226
17	1.12798039995306	0.16993386409437	−0.02304096729203	0.00347119346741	0.00091515473431	2.5585229
25	1.12798040098244	0.16993386632558	−0.02304097349784	0.00347119642486	0.00091515689483	2.5585231
33	1.12798040105726	0.16993386650219	−0.02304097400496	0.00347119667242	0.00091515710753	2.5585226
41	1.12798040105939	0.16993386650225	−0.02304097399348	0.00347119665821	0.00091515709910	2.5585231
49	1.12798038900362	0.16993384321933	−0.02304098436389	0.00347122011103	0.00091522372105	2.5556215

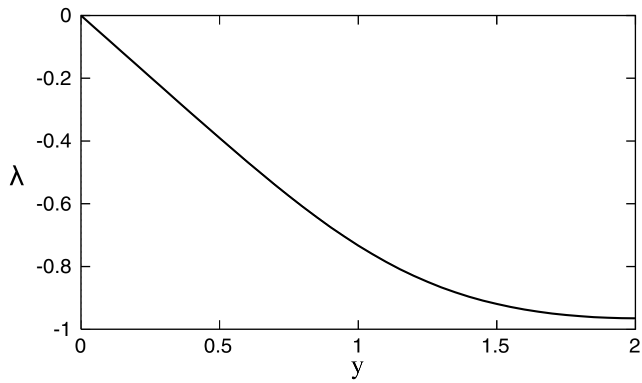

Fig. 3. Calculated Lagrange multipliers with $N_\alpha = 60$ and $N_\lambda = 41$.

tions characterized by the asymptotic expansion in terms of the eigenpairs (which are computed using a modified Steklov method). See [8,9] for details.

The computations were performed using the commercial FEM package STRESSCHECK (E.S.R.D. St. Louis, MO) on an IBM Pentium III machine. Since this is a p version package, the geometrically graded mesh was constructed a priori and the polynomial shape functions were taken to have degree $p = 1,\ldots,8$, uniformly over all elements in the (fixed) mesh. The CPU time was approximately 9 s for the calculation of u_{FEM} and about 2 s for the calculation of the α_j's. Table 4 shows the potential energy as well as the (estimated) percentage relative error in the energy norm,

$$\mathrm{Error} = 100 \times \frac{\|u_{\mathrm{EX}} - u_{\mathrm{FEM}}\|_{E(\Omega)}}{\|u_{\mathrm{EX}}\|_{E(\Omega)}},$$

indicating that u_{FEM} is computed accurately. Table 5 shows the computed singular coefficients, which were obtained using u_{FEM} corresponding to $p = 8$. These results show that the p version of the FEM (on geometrically graded meshes) seems to perform quite well when compared with the results obtained using other methods found in the literature.

The capacitance, C, was calculated from the solution corresponding to $p = 8$. Since u_{FEM} is a polynomial of degree 8 in x and y, we see from (20) that a 5-point Gaussian quadrature formula is sufficient to exactly evaluate the integral involved. We obtained $C_{\mathrm{FEM}} = 2.557256$, an approximation which is not as good as that obtained using the SFBIM. We believe this is due to the *pollution* effects that are influencing the extraction of the data of interest (see e.g. [1]). Pollution is a phenomenon that occurs when singularities are present in the solution of an elliptic boundary value problem. These singularities cause the numerical method to yield inaccurate results *away* from the point of singu-

Table 2
Convergence of the solution with N_α; SFBIM with $N_\lambda = 41$

N_α	α_1	α_2	α_3	α_4	α_5	C
45	1.12798046929652	0.16993391450191	−0.02304128110013	0.00347021000332	0.00091337482002	2.5467734
50	1.12798040111620	0.16993386693468	−0.02304097583682	0.00347118005697	0.00091509465304	2.5585230
55	1.12798040105939	0.16993386650225	−0.02304097399348	0.00347119665822	0.00091515709909	2.5585231
60	1.12798040105939	0.16993386650225	−0.02304097399348	0.00347119665821	0.00091515709910	2.5585231
65	1.12798040105939	0.16993386650223	−0.02304097399351	0.00347119665821	0.00091515709917	2.5585231
70	1.12798040105938	0.16993386650176	−0.02304097399413	0.00347119665866	0.00091515710049	2.5585230
75	1.12798040105929	0.16993386650304	−0.02304097399577	0.00347119665730	0.00091515709264	2.5585230
80	1.12798040105953	0.16993386650246	−0.02304097399337	0.00347119665919	0.00091515710302	2.5585232

Table 3
Converged values of the singular coefficients; SFBIM with N_λ=41 and $N_\alpha = 60$

i	α_i	Ref. [14]
1	1.12798040105939	1.1280
2	0.16993386650225	0.1699
3	−0.02304097399348	−0.0230
4	0.0034711966582	0.0035
5	0.0009151570991	0.0009
6	−0.0001128038345	
7	0.0000877165245	
8	0.0000277603137	
9	−0.0000044161578	
10	0.0000027539457	
11	0.0000009219619	
12	−0.0000001554459	
13	0.0000001088408	
14	0.0000000379699	
15	−0.0000000066619	
16	0.000000004711	
17	0.00000000168	
18	−0.00000000030	
19	0.00000000022	
20	0.00000000008	
C	2.5585231	2.5585

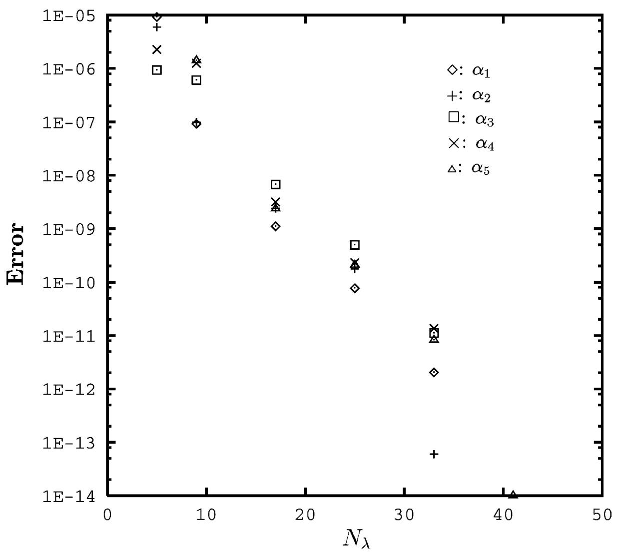

Fig. 4. Convergence of the SFBIM with N_λ; $N_\alpha = 60$.

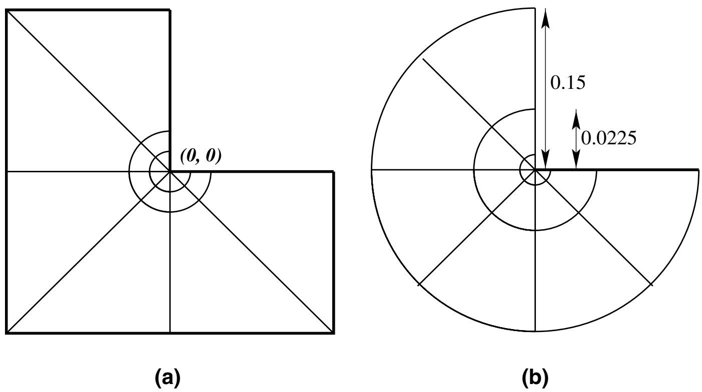

Fig. 5. (a) Geometrically graded mesh over the domain Ω; (b) Mesh detail near the re-entrant corner.

Table 4
Values of the potential energy and the percentage relative error in the *p*/*hp* method

p	DOF	Energy	Error (%)
1	10	1.3385078	21.52
2	39	1.2819648	4.60
3	74	1.2806200	3.26
4	127	1.2793571	0.85
5	198	1.2792877	0.43
6	287	1.2792738	0.28
7	394	1.2792690	0.20
8	519	1.2792667	0.15

Table 5
Values of the leading singular coefficients obtained with the *p*/*hp* method

i	α_i, DOF = 519	α_i, DOF = 691
1	1.12797960	1.12798010
2	0.16993396	0.16993387
3	−0.0230434	−0.0230419
4	−0.0034780	−0.0034755
5	0.0009115	0.0009126
C	2.557256	2.558588

larity (as is the case here), when certain quantities of engineering interest are computed. The *p* version of the FEM is much more susceptible to pollution effects than the *h* and *hp* versions. We repeated the calculation using a more refined mesh near the re-entrant corner, as seen in Fig. 6. The newly computed

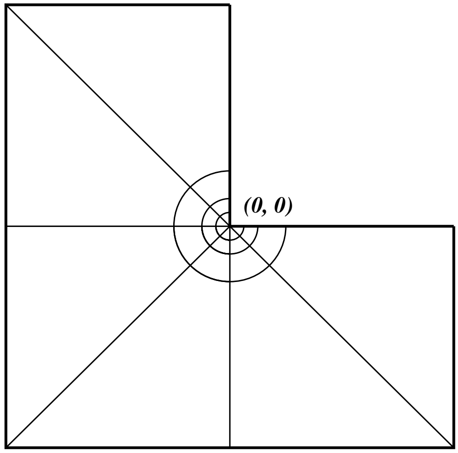

Fig. 6. Refined mesh.

singular coefficients are shown in Table 5 and the capacitance is recomputed as $C_{\mathrm{FEM}} = 2.558588$, which is a much better approximation. The refined mesh required 691 degrees of freedom (for $p = 8$), as opposed to 519 used before, and the CPU time increased by 1 s.

6. Conclusions

We have solved a Laplacian problem over an *L*-shaped domain using both the SFBIM and the *p*/*hp* finite element method, and studied the convergence of the solution with the numbers of singular functions and of Lagrange multipliers, and the number of degrees of freedom, respectively. With the SFBIM the leading singular coefficients of the local singularity expansion are calculated explicitly, whereas with the *p*/*hp*-FEM they are calculated by post-processing the numerical solution.

Fast convergence is achieved and highly accurate results are obtained with both methods, which perform considerably better than other techniques found in the literature (e.g. that of Igarashi and Honma [14]). Given that there are no known exact values for the singular coefficients, the very good agreement between the SFBIM and the *p*/*hp* FEM serves as *validation* for the computational results presented here. We should point out that, in terms of efficiency, the SFBIM is a better choice, since the singular coefficients are computed directly and no post-processing is necessary. On the other hand, the FEM can be applied to a much wider class of problems than those that can efficiently and effectively be handled by the SFBIM. We should mention that currently there is no mathematical theory that establishes the observed exponential convergence rate of the SFBIM; this is the focus of our current research efforts.

References

[1] B. Szabó, I. Babuška, Finite Element Analysis, John Wiley & Sons Inc., New York, 1991.
[2] M. Arad, Z. Yosibash et al., Comparing the flux intensity factors by a boundary element method for elliptic equations with singularities, Commun. Numer. Meth. Eng. 14 (1998) 657–670.
[3] Z.-C. Li, T.T. Lu, Singularities and treatments of elliptic boundary value problems, Math. Comput. Model. 31 (2000) 97–145.
[4] N.K. Mukhopadhyay, S.K. Maiti, A. Kakodkar, A review of SIF evaluation and modelling of singularities in BEM, Comput. Mech. 25 (2000) 358–375.
[5] I. Babuška, B. Guo, The *h–p* version of the finite element method. Part I: the basic approximation results, Comput. Mech. 1 (1986) 21–41.
[6] I. Babuška, A. Miller, The post-processing approach in the finite element method – Part 1: calculation of displacements, stresses and other higher derivatives of the displacements, Int. J. Numer. Meth. Eng. 20 (1984) 1085–1109.
[7] I. Babuška, A. Miller, The post-processing approach in the finite element method – Part 2: the calculation of stress intensity factors, Int. J. Numer. Meth. Eng. 20 (1984) 1111–1129.
[8] B.A. Szabó, Z. Yosibash, Numerical analysis of singularities in two dimensions. Part 1: computation of the eigenpairs, Int. J. Numer. Meth. Eng. 38 (1995) 2055–2082.
[9] B.A. Szabó, Z. Yosibash, Numerical analysis of singularities in two dimensions. Part 2: computation of generalized flux/stress intensity factors, Int. J. Numer. Meth. Eng. 39 (1996) 409–434.
[10] S.C. Brenner, Multigrid methods for the computation of singular solutions and stress intensity factors I: corner singularities, Math. Comput. 68 (1999) 559–583.
[11] G.C. Georgiou, L.G. Olson, Y. Smyrlis, A singular function boundary integral method for the Laplace equation, Commun. Numer. Meth. Eng. 12 (1996) 127–134.
[12] G.C. Georgiou, A. Boudouvis, A. Poullikkas, Comparison of two methods for the computation of singular solutions in elliptic problems, J. Comput. Appl. Math. 79 (1997) 277–290.
[13] M. Elliotis, G. Georgiou, C. Xenophontos, The solution of a Laplacian problem over an L-shaped domain with a singular function boundary integral method, Comm. Numer. Meth. Eng. 18 (2002) 213–222.
[14] H. Igarashi, T. Honma, A boundary element method for potential fields with corner singularities, Appl. Math. Model. 20 (1996) 847–852.
[15] G.T. Symm, Treatment of singularities in the solution of Laplace's equation by an integral equation method, National Physical Laboratory Report NAC31, 1973.
[16] P. Grisvard, Elliptic Problems in Nonsmooth Domains, Pitman Publishers, England, 1995.
[17] Z.-C. Li, R. Mathon, P. Sermer, Boundary methods for solving elliptic problems with singularities and interfaces, SIAM J. Numer. Anal. 24 (1987) 487–498.